Proc. of the 8th International Conference NEET 2013, Zakopane, Poland, June 18–21, 2013

Elemental Composition, Topography and Wettability of $Pb_xSn_{1-x}S$ Thin Films

I.S. Tashlykov[a,*], A.I. Turavets[a], V.F. Gremenok[b] and P. Żukowski[c]

[a]Belarusian State Pedagogical University, Minsk, Belarus

[b]Scientific and Practical Materials Research Centre of the NAS of Belarus, Minsk, Belarus

[c]Lublin University of Technology, Lublin, Poland

PbSnS thin films were prepared by hot-wall vacuum evaporation. The Rutherford backscattering technique was employed for the investigation of $Pb_xSn_{1-x}S$ thin films composition. With a help of atomic force microscopy the main stages in the development of the thin films were characterized. Contact angle measurements of water drop on $Pb_xSn_{1-x}S$ thin films have been conducted on our original setup.

DOI: 10.12693/APhysPolA.125.1339

PACS: 68.37.Ps, 06.30.Bp

1. Introduction

Ternary semiconductor materials have attracted much attention because of their potential application in photonic devices [1]. PbS–SnS materials are promising materials in photovoltaic, infrared detection [2]. In addition, by using tin sulfide compounds in photovoltaic structures the production costs of solar cells would decrease, because the materials involved are cheap, nonstrategic, and abundant in nature.

As we know, the fabrication involves many steps, using different deposition methods. It is usually a time consuming and expensive process. In general, the nature of the surface of any material plays a crucial role in device fabrication. The surface energy of the adhesive material and the contact angle are the characteristics of molecular adhesion. Sufficient wetting is necessary for a good contact adhesion. The larger the wetting, and hence, the smaller contact angle, the stronger the adhesion and the greater the possibility for the adhesive material filling the pores on the surface of the substrate. If the adhesive material in the coating formed air bubbles between the adhesive and the substrate, then these areas are potentially breaking the adhesive bonds in some places as a result of the applied external force. Therefore, the performance of the junction and the cell depends critically on composition, structure and morphology of the absorber surface, whereas local inhomogeneity, chemical composition and surface morphology determine surface wettability. The wettability interferes with adhesion absorber surface [3] (and, in turn, with performance of the junction), which in turn influences solar cell energy conversion efficiency. Lokhande et al. [4] and Roh et al. [5] propose to use contact angle measurements as a diagnostic method to determine the quality of $CuInS_2$ absorbers without forming an actual solar cell.

*corresponding author; e-mail: tashl@bspu.unibel.by

The purpose of this project is to study morphology and wettability of the surface of $Pb_xSn_{1-x}S$ films fabricated in a wide temperature range. We use hot wall technique for synthesis of polycrystalline thin films on glass substrates. For the synthesis, the substrate temperature was varied. Surface properties of thin films were studied by using atomic force microscopy (AFM) and contact angle measurements.

2. Experiment details

The polycrystalline $Pb_xSn_{1-x}S$ ingots used as a source material were synthesized by reaction of stoichiometric mixtures of pure Sn and S (99.99%) and natural galena (PbS). The mixture is sealed under 1.3×10^{-1} Pa vacuum in quartz tube. It was placed vertically in an electric furnace and kept at 450 °C for 7 days and after that at 700 °C for 10 days. In order to avoid explosions due to the sulfur vapour pressure, the tube was heated slowly (25 °C/h). Then the product was ground and mixed in an agate mortar, sealed in a silica glass tube and reheated at 700 °C for 10 days. Crushed powder was used as raw material for the hot wall vacuum evaporation (Fig. 1) onto glass slides and molybdenum boat was used as evaporator. The chamber pressure was about 3×10^{-4} Pa. Substrates were chemically cleaned, rinsed with water and blown dry with compressed air before deposition. The substrate temperature was measured using a chromel–alumel thermocouple in contact with substrate surface. Substrate and wall temperatures were 200 °C–382 °C and 600 °C, respectively. The distance between source and substrate has been maintained as constant at 12 cm, deposition time was 30 min.

Atomic force microscopy (AFM) study of samples was performed with an atomic force microscope "NT-206" using cantilevers CSC21. Roughness values in this paper refer to the average surface roughness values, R_a. The roughness ratio k is defined as the ratio of true area of the solid surface to the apparent area. AFM images were analyzed using the SurfaceXplore 1.3.11 program.

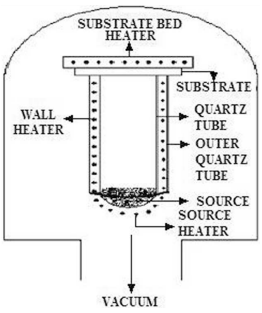

Fig. 1. Schematic diagram of a hot wall deposition system.

The wetting behavior is characterized by a value of the contact angle (Θ_0). Contact angle measurements were based on the sessile-drop method described in [6]. The wetting agent was doubly distilled water. Besides contact angle measurements based on the sessile-drop method contact angle hysteresis evaluation was conducted by extension/contraction method. We measure the contact angle in the state in which the droplet is attached to both the needle tip and solid surface, and the droplet amount is increased or decreased. The angle formed while increasing volume is called the advancing angle (Θ_a), likewise the angle while decreasing volume is called the receding angle (Θ_r). Contact angle hysteresis is defined as the difference between advancing and receding angles: $\Delta\Theta = \Theta_a - \Theta_r$.

The wetting of rough textured surfaces can be described by models: Wenzel, Cassie–Baxter, liquid film state. The Wenzel model describes homogeneous wetting regime (when the liquid fills in the roughness grooves of a surface). In the case when the liquid does not fill in the roughness grooves of a surface, the Wenzel model is not sufficient. The drop of water creates on the substrate small air pockets underneath it. It is a heterogeneous wetting regime and surface is a composite of two types of patches: air and solid. This heterogeneous surface is explained using the Cassie–Baxter model. The Wenzel state switches to the liquid film state when the penetration front spreads beyond the drop and a liquid film forms over the surface. The film smoothes the surface roughness and the Wenzel model no longer applies.

The Rutherford backscattering technique was employed for the investigation of target composition and for depth profiling of components in films. The energy of He^+ ions was 1.5 or 2.0 MeV, and the scattering, entry and escape angles were 160°, 0°, and 20°, respectively. The energy resolution of the analyzing system was 15 keV. Concentration profiles of components were evaluated using the RUMP code computer simulation. However, the quantitative application of that method is restricted to laterally homogeneous and smooth films. Surface roughness, such as grains, can cause diffusion-like broadening of the spectrum and it is difficult to render the interpretation of the result. The effect of rough films on a smooth substrate was investigated by Mayer [7]. The effect of layer roughness on the shape of RBS spectra was investigated for incident He^+ ions backscattered from a gold layer at a scattering angle of 165°. In RBS geometry, the layer roughness results in broadening of the low energy edge of thin films and the development of tails stretching to low energies.

3. Results and discussion

Some AFM images of the $Pb_xSn_{1-x}S$ films are shown in Fig. 2. These pictures indicate how the shape of the surface changes with an increase of substrate temperature. The topography and wettability parameters are listed in Table I.

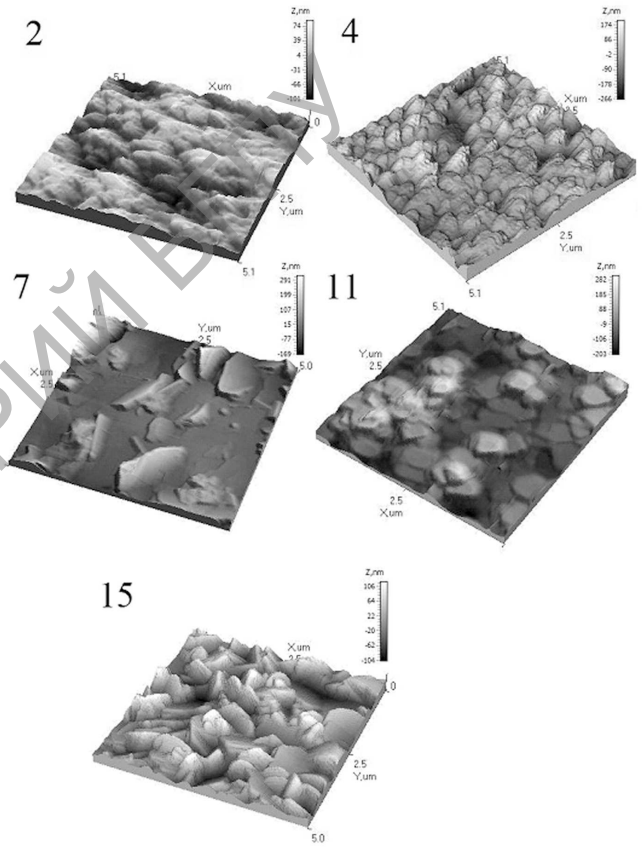

Fig. 2. AFM pictures (3D) of $Pb_xSn_{1-x}S$ samples deposited at different substrate temperatures T_s: 2 — $T_s = 206\,^\circ C$, 4 — $T_s = 240\,^\circ C$; 7 — $T_s = 290\,^\circ C$; 11 — $T_s = 320\,^\circ C$; 15 — $T_s = 330\,^\circ C$.

We can identify and describe the main types of thin films synthesized at different substrate temperatures. Group 1 consists of samples 1, 2, 3, 8. They are united by the disorder of the crystallites on the surface, the absence of a specific shape, size and orientation of crystallites. The samples are composed of vertically placed crystallites. With increasing T_s crystallites become more developed, the density of their distribution is reduced. It

TABLE I

Topography and wettability parameters of $Pb_xSn_{1-x}S$ thin films.

No.	T_s [°C]	R_a [nm]	k	f	Θ [°]	Θ_c^1 [°]	Θ_c^2 [°]	Wenzel Θ [°]
1	200	18.5	1.009	0.592	119.0	168.1	11.9	118.7
2	206	23.6	1.007	0.507	79.8	170.4	9.6	79.9
3	210	42.1	1.043	0.620	50.0	153.9	26.1	52.0
4	240	47.0	1.020	0.621	125.4	161.6	18.4	124.6
5	268	14.0	1.001	0.698	70.7	175.3	4.7	70.7
6	280	16.9	1.031	0.647	98.4	156.8	23.2	98.1
7	290	70.9	1.074	0.830	107.6	134.2	45.8	106.4
8	300	116.0	1.049	0.726	40.9	147.9	32.1	43.9
9	302	37.7	1.024	0.745	82.7	156.1	23.9	82.9
10	319	36.7	1.037	0.746	93.9	150.8	29.2	93.8
11	320	69.3	1.048	0.744	82.0	147.4	32.6	82.4
12	320	70.5	1.059	0.764	94.5	143.1	36.9	94.2
13	325	18.8	1.004	0.759	78.7	169.6	10.4	78.7
14	330	107.8	1.113	0.684	95.0	137.4	42.6	94.5
15	330	32.2	1.054	0.637	100.7	150.5	29.5	100.1
16	361	56.7	1.036	0.731	113.0	151.9	28.1	112.2
17	382	240.6	1.216	0.774	117.9	120.8	59.2	112.6

can be seen that the size of the largest crystallites and R_a increase with T_s increasing, because of the sintering, wherein small grains coalesce to form larger grains.

Group 2 consists of samples 4 and 6. These films consist of vertically placed crystals of approximately the same shape and size. It also appears that the grown granules are loosely packed together and form a highly rough surface. The crystallite size, the R_a of the films decreases with increasing T_s.

The third group consists of film 5, 7, 10, 12, 13. The entire deposited material is subdivided into a more or less continuous layer and crystallites grown on it. The main film consists of stacked blocks with their c-axis always parallel to growth direction. The size of the blocks is different for the different samples and has no clear dependence on the temperature of the substrate. The crystallites grown on the surface of the films have the geometric shape: rectangular blocks for lower temperatures, and the pyramid to the higher temperature of the substrate.

Samples 9, 11, 16 can also be counted to the Group 3, but we distinguish them in a separate Group 4. Their difference is that the nanorods (whiskers) grow on the surface of the film. Thin film 9 has few droplets on its surface only. Such droplets were already observed on the surface of PbS, PbTe, PbSe thin films prepared by hot-wall vacuum evaporation (HWVE) [8].

The last group 5 consists of the samples 14, 15, 17. Ordered placement of blocks in these films (as in groups 3 and 4) is replaced by a disordered one. The crystals on the surface of films are placed randomly and undirected. There is no definite shape and size of the crystallites.

The images of the all thin films showed a densely packed microstructure free of pinholes. The grains are well connected with each other, which is essential for the development of p–n junction.

Figure 3 shows the position of a water drop on the surface of $Pb_xSn_{1-x}S$ samples.

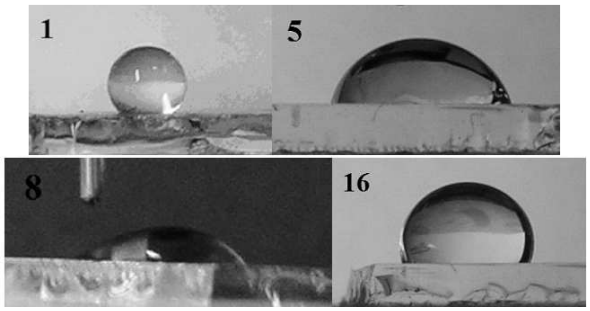

Fig. 3. Water drop on surfaces of $Pb_xSn_{1-x}S$ deposited at different substrate temperatures T_s: 1 — $T_s = 200\,°C$; 5 — $T_s = 268\,°C$; 8 — $T_s = 300\,°C$; 16 — $T_s = 361\,°C$.

We consider two factors affecting the wettability of the surface: elemental composition and topography. Due to the nature of the method of producing thin films, we can neglect the chemical inhomogeneity of the samples. At first, let us analyze which model should be applied to describe the wettability of rough thin films. Let us find a critical wetting angle. The critical contact angles Θ_c^1 and Θ_c^2 can be found after estimation of the part f of the total surface area wet by the liquid. f was estimated using the "SurfaceXplore" and "Gwyddion" programs with a help of histograms of the height distribution. The level of water penetration into the pores between the crystallites is defined around the assumption that this level is below the most common height of the crystallite. Further, we find Θ_0 using three proposed formulae for all films:

$$\cos\Theta = f\cos\Theta_0 + 1 - f \quad \text{(liquid film state)},$$

$$\cos\Theta = k\cos\Theta_0 \quad \text{(Wenzel state)},$$

$$\cos\Theta = f\cos\Theta_0 + f - 1 \quad \text{(Cassie state)}.$$

We found that only for the Wenzel formula the contact angle Θ_0 is in the interval of $\Theta_c^2 < \Theta_0 < \Theta_c^1$. For the other formulae Θ_0 is outside the respective regions $0 < \Theta_0 < \Theta_c^2$ and $\Theta_c^1 < \Theta_0 < 180°$. Based on these calculations, we use the Wenzel model to describe the wettability of our films; i.e. drop of water do not form air bubbles between the water and the substrate (the Wenzel model definition). The relative deviation of the Wenzel formula contact angle from the experimentally measured Θ range from -4.5% to 7.4%.

In some cases, the Cassie model can work outside $\Theta_c^1 < \Theta_0 < 180°$ [9]. After the first results of the $Pb_xSn_{1-x}S$ samples water wettability investigation, questions were raised about the applicability of the Wenzel model to samples 4, 6, 9, 11, 16, which consist of stacked blocks with their c-axis parallel to the growth direction and the crystallites (pyramids or whiskers) grown on it.

To check the results, studies of the contact angle hysteresis of water drop have been conducted. The contact

angles in both states are comparable (the Wenzel angle is slightly smaller than the Cassie one), but the hysteresis is dramatically affected by the change of state: it is found to be 10–20 times larger in the Wenzel regime. This is a sign of air trapping: because the drop sits on a cushion of air, its pinning on the solid (which is responsible for the hysteresis) is highly reduced [10]. In the case of Cassie model, perimeter of contact between the drop and the surface immediately begins to decrease at contraction of the drop.

The surface of the thin films will be characterized by a dimensionless quantity L/H, where L — the maximum distance between the columns within a single unit cell texture, and H — height of the columns. Texture coefficient L/H determines whether the meniscus of the liquid touches the lower surface of texture. Their relationship predicts the existence and the transition from the Wenzel model to the Cassie model.

TABLE II

Values of the advancing, receding, and hysteresis contact angles, and texture coefficient of $Pb_xSn_{1-x}S$ samples.

No.	Θ_r [°]	Θ_a [°]	$\Delta\Theta$ [°]	L/H
4	40.5	127.0	86.50	1.02
6	37.6	101.3	63.70	2.94
9	32.3	86.1	53.80	4.00
11	48.6	84.0	35.40	5.06
16	30.0	113.5	83.50	2.50

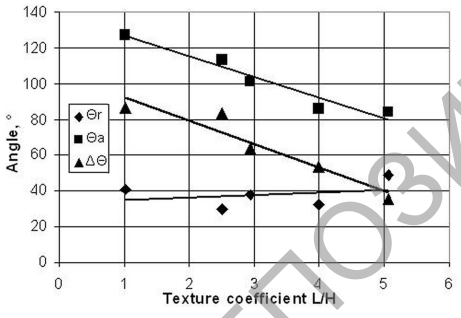

Fig. 4. Values of the advancing, receding, and hysteresis contact angles as a function of the texture coefficient.

The values of the receding contact angles look almost independent from the texture coefficient, while the value of the advancing contact angle decreases with increasing texture coefficient (Table II and Fig. 4). $\Delta\Theta$ therefore decreases with increasing period texture. The contact angle hysteresis of the samples is not less than 35.4°, hence we must use the model Wenzel description of their wettability.

In experiments [11] it has been shown that for a glass substrate $R_a = 2.2$ nm, and the thickness of the $Pb_xSn_{1-x}S$ films, whose chemical composition was investigated by means of RBS and RUMP, is more than 830 nm. Thus, substrates can be considered to be smooth, because of their roughness is much smaller than the mean thickness d of the film. By means of the program "SurfaceXplore" we estimated values of mean thickness d and standard deviation σ for samples 5, 7, 12, 15, 16, 17 (Table III).

TABLE III

Atomic composition, mean thickness value and standard deviation of the $Pb_xSn_{1-x}S$ films.

No.	T_s [°C]	The maintenance of elements [at.%]		D [nm]	σ [nm]	σ/d
5	268	Sn Pb S	37.3 10.4 52.3	830	21.5	0.03
7	290	Sn Pb S	39 7.6 53.4	900	89.7	0.10
12	320	Sn Pb S	38 9.5 52.5	950	106.6	0.11
15	330	Sn Pb S	40.2 6.8 53	1160	37.9	0.03
16	361	Sn Pb S	43.4 8.6 48	1680	68.7	0.04
17	382	Sn Pb S	39 8.3 52.7	1150	283.5	0.25

In our case the thickness variation is much smaller than the mean film thickness. Comparing the calculated results with Mayer's results (energy spectra for 2 MeV ^{4}He backscattered from a smooth and rough gold layers with mean thickness 1×10^{18} cm^{-2} and different roughnesses with standard deviation σ) we can conclude that only the low energy edge of the film is affected by the roughness and gets broader. The development of tails stretching to low energies is negligible. In our RBS spectra, the surface roughness can cause an error in evaluating elemental composition deeply in a simulated film (in the intermediate layer of elements of a substrate and a coating).

The energy spectrum of 2 MeV ^{4}He backscattered from rough $Pb_xSn_{1-x}S$ films deposited on glass is shown in Fig. 5. The experimental data are not well reproduced by the simulated spectrum, especially the small background. The remaining discrepancies between experimental data and simulation are mainly due to plural scattering, which was not taken into account in the calculation. The typical depth profile for one representative sample is given in Fig. 6. The depth profiles of films reveal relatively uniform distribution of components in the bulk of the films through the depth. Table III contains the average atomic concentrations of Pb, Sn and S determined for the films.

The $Pb_xSn_{1-x}S$ films are 0.83–1.68 μm thick (at different temperatures). With the increase of the substrate

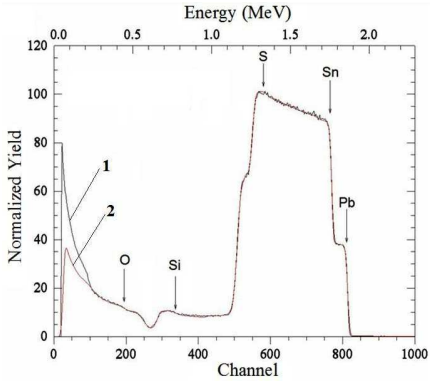

Fig. 5. 2.0 MeV He^+ RBS spectra from PbSnS film (sample 5) deposited at $T_{sub} = 268\,^{\circ}C$: 1 — experimental data; 2 — simulation.

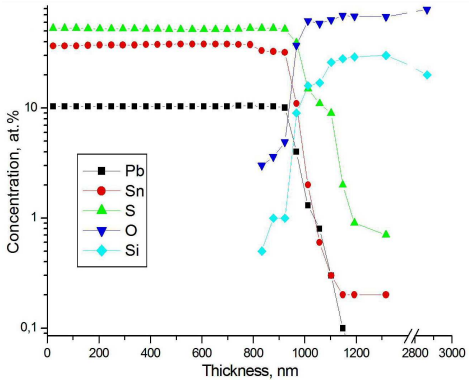

Fig. 6. Depth distribution of species in PbSnS film (sample 5) deposited at $T_{sub} = 268\,^{\circ}C$.

temperature, the thickness of a film increases, too. The films consist of 6.8–10.4 at.% of lead, 37.3–43.4 at.% of tin, 48.0–53.4 at.% of sulphur. Profiles of element distribution show that the obtained films are homogeneous.

The depth profiles indicate that noticeable amounts of lead, tin, and sulphur penetrate in the depth more than 0.5 μm under the interface between the thin film and a substrate. This means that during HWVD process the Pb, Sn, and S atoms penetrate deeply into the glass. The thickness of an intermediate layer is from 0.48 μm to above 1.65 μm for different samples. As appears from the spectra, the substrate contains silicon and oxygen atoms. One can observe outdiffusion of elements from the substrate into the coating.

4. Conclusions

With a help of AFM the main stages in the development of the thin films have been investigated.

We have proposed a possible description of the wetting (or dewetting) of a rough textured surface with two parameters: the roughness ratio k and the part f of the total surface area wet by the liquid. The effective contact angle Θ could be calculated on such a surface, as a function of these parameters and the Young contact angle, fixed by the chemical nature of the solid and the liquid.

The studies of the contact angle hysteresis of water drop have been conducted in order to confirm the validity of using the Wenzel model in description of the water wettability of $Pb_xSn_{1-x}S$ films. The values of the receding contact angles look almost independent of the texture coefficient, while the value of the advancing contact angle decreases with increasing texture coefficient. Contact angle hysteresis decreases with increasing texture coefficient.

The $Pb_xSn_{1-x}S$ films are 0.83–1.68 μm thick (at different temperatures). With the increase of the substrate temperature, the thickness of films increases, too. Profiles of distribution of elements show that the obtained films are homogeneous. As appears from spectra, the substrate includes silicon and oxygen. Mutual diffusion of elements of a substrate (Si, O) and a coating (Pb, Sn, S) has been observed. The thickness of an interphase layer is from 0.48 μm to above 1.65 μm for different samples.

References

[1] A. Goetzberger, C. Hebling, H.W. Schock, *Mater. Sci. Eng.* **R40**, 1 (2003).

[2] R.H. Bube, *Photoconductivity of Solids*, Wiley, New York 1960, p. 234.

[3] W.A. Zisman, *Contact Angle Wettabil. Adhes.* **43**, 1 (1964).

[4] C.D. Lokhande, A. Barkschat, H. Tributsch, *Solar Energy Mater. Solar Cells* **79**, 293 (2003).

[5] S.J. Roh, R.S. Mane, H.M. Pathan, O.-S. Joo, S.-H. Han, *Appl. Surf. Sci.* **252**, 1981 (2005).

[6] I. Tashlykov, A. Turavets, P. Zukowski, *Acta Phys. Pol. A* **123**, 840 (2013).

[7] M. Mayer, *Nucl. Instrum. Methods Phys. Res.* **194**, 177 (2002).

[8] A. Lopez-Otero, L.D. Haas, *Thin Solid Films* **23**, 1 (1974).

[9] A. Lafuma, D. Quéré, *Nature Mater.* **2**, 457 (2003).

[10] R.E. Johnson, R.H. Dettre, *Contact Angle Wettabil., Adhes. Adv. Chem.* **43**, 112 (1964).

[11] A.I. Turavets, I.S. Tashlykov, O.G. Bobrovich, in: *XXXXII Int. Conf. on Physics of Interaction of Charged Particles with Crystals*, Ed.: M.I. Panasiuk, University Book, Moscow 2012, p. 152.